

RESEARCH

Open Access



Different photosynthetic responses of haploid and diploid *Emiliana huxleyi* (Prymnesiophyceae) to high light and ultraviolet radiation

Zuoxi Ruan¹, Meifang Lu¹, Hongmin Lin⁵, Shanwen Chen¹, Ping Li^{1,4}, Weizhou Chen¹, Huijuan Xu^{2*} and Dajun Qiu^{3*}

Abstract

Solar radiation varies quantitatively and qualitatively while penetrating through the seawater column and thus is one of the most important environmental factors shaping the vertical distribution pattern of phytoplankton. The haploid and diploid life-cycle phases of coccolithophores might have different vertical distribution preferences. Therefore, the two phases respond differently to high solar photosynthetically active radiation (PAR, 400–700 nm) and ultraviolet radiation (UVR, 280–400 nm). To test this, the haploid and diploid *Emiliana huxleyi* were exposed to oversaturating irradiance. In the presence of PAR alone, the effective quantum yield was reduced by 10% more due to the higher damage rate of photosystem II in haploid cells than in diploid cells. The addition of UVR resulted in further inhibition of the quantum yield for both haploid and diploid cells in the first 25 min, partly because of the increased damage of photosystem II. Intriguingly, this UVR-induced inhibition of the haploid cells completely recovered half an hour later. This recovery was confirmed by the comparable maximum quantum yields, maximum relative electron transport rates and yields of the haploid cells treated with PAR and PAR+UVR. Our data indicated that photosynthesis of the haploid phase was more sensitive to high visible light than the diploid phase but resistant to UVR-induced inhibition, reflecting the ecological niches to which this species adapts.

Keywords *Emiliana huxleyi*, Diploid phase, Haploid phase, Effective quantum yield, Ultraviolet radiation (UVR)

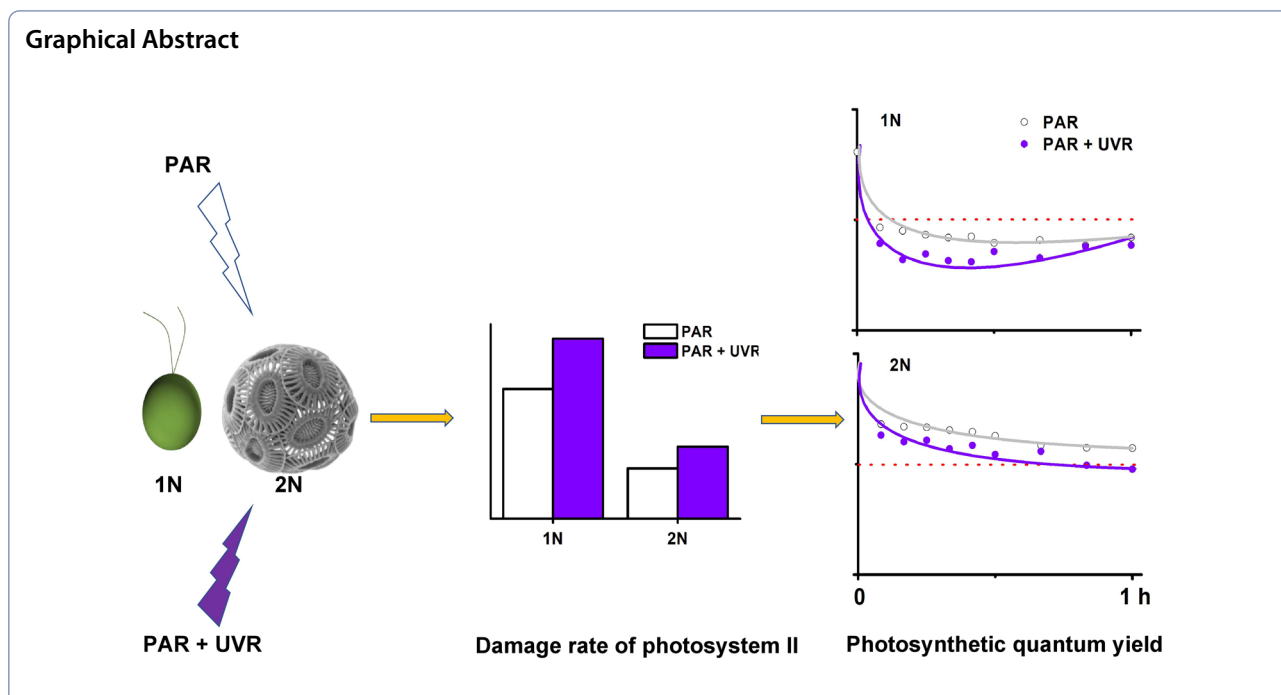
*Correspondence:

Huijuan Xu
xuhj@ms.giec.ac.cn
Dajun Qiu
djqu@scsio.ac.cn

Full list of author information is available at the end of the article



© The Author(s) 2023. **Open Access** This article is licensed under a Creative Commons Attribution 4.0 International License, which permits use, sharing, adaptation, distribution and reproduction in any medium or format, as long as you give appropriate credit to the original author(s) and the source, provide a link to the Creative Commons licence, and indicate if changes were made. The images or other third party material in this article are included in the article's Creative Commons licence, unless indicated otherwise in a credit line to the material. If material is not included in the article's Creative Commons licence and your intended use is not permitted by statutory regulation or exceeds the permitted use, you will need to obtain permission directly from the copyright holder. To view a copy of this licence, visit <http://creativecommons.org/licenses/by/4.0/>.



Introduction

Coccolithophores are often covered with one or several layers of calcareous plates (i.e. coccoliths) around the cell surface. As one of the most important groups of marine phytoplankton, coccolithophores, together with other main calcifiers (e.g. foraminifera), account for almost half of the total production of CaCO_3 in the pelagic zone (Balch et al. 2007; Brownlee et al. 2021). Therefore, they are of great importance in regulating the global biogeochemical carbon cycle.

Emiliania huxleyi is the most successful species of coccolithophores in the present-day ocean. It is frequently the dominant phytoplankton species in terms of cell number in surface seawater. More importantly, *E. huxleyi* forms extensive blooms with a large number of cells, and these blooms cover up to $1.4 \times 10^6 \text{ km}^2$ of the world ocean annually (Holligan et al. 1993; Brown and Yoder 1994; Tyrrell and Merico 2004; Brownlee et al. 2021). Several environmental factors, including low silicate contents, high carbonate saturation state, etc., are considered facilitative for the development of blooms (Tyrrell and Merico 2004; Zondervan 2007; Pozdnyakov et al. 2021). However, high light conditions seem to be a crucial prerequisite for blooms (Tyrrell and Merico 2004; de Vries et al. 2020). At the sea surface or the water column surface, a high intensity of photosynthetically active radiation (PAR, 400–700 nm) is always accompanied by a high intensity of ultraviolet radiation (UVR, 280–400 nm), known as a stress factor damaging the protein and DNA

of phytoplankton (Sinha and Häder 2002; Leunert et al. 2014; Haney et al. 2022). Depending on the scattering and absorption of seawater, UVR might penetrate through the water column to a depth of more than 20 m, where *E. huxleyi* is often observed and its blooms tend to occur (Nanninga and Tyrrell 1996; Falkowski and Raven 1997; Boelen et al. 1999; Frada et al. 2012; Jin et al. 2013; Pozdnyakov et al. 2021). *E. huxleyi* is thus expected to be exposed to UVR, especially if the vertical mixing of surface water is also considered (Jin et al. 2013).

The life cycle of *E. huxleyi* is typically composed of a diploid (2N) phase with coccolith-bearing or naked (without coccoliths) cells and a haploid (1N) phase with organic scale-bearing cells; both phases may propagate independently by mitosis (Green et al. 1996; Frada and Vardi 2017). The haploid and diploid phases of coccolithophores (e.g. *Calcidiscus leptoporus*, *Coccolithus pelagicus*) frequently concentrate in the upper photic zone during blooms (Frada et al. 2012; D’Amario et al. 2017). Although the diploid *E. huxleyi* can endure high light and does not show photoinhibition, even at $1000 \mu\text{mol photons m}^{-2} \text{ s}^{-1}$ (Nanninga and Tyrrell 1996), it seems to be susceptible to UVR in terms of growth, photosynthesis, and calcification (Buma et al. 2000; van Rijssel and Buma 2002; Gao et al. 2009; Guan and Gao 2010a, b; Jin et al. 2022), which is similar to that observed for certain chlorophytes and diatoms (Lorenzo et al. 2019; Zang et al. 2022). Calcification, which is only found in diploid cells, may consume a significant part of the cell energy budget,

mainly due to active ion transportation and coccolith polysaccharide production (Anning et al. 1996; Kayano and Shiraiwa 2009; Kayano et al. 2011; Monteiro et al. 2016; Vázquez et al. 2022). Such behaviour appears critical for the cells to avoid photodamage and maintain a relatively high photosynthesis performance, e.g. when cells are exposed to an abrupt increase in irradiance (Guan and Gao 2010a, b; Ramos et al. 2012; Xu et al. 2016). Coccoliths have also been shown to remove a considerable part of PAR and UVR, especially UVR-B, and they may also play a role in protecting the cell against high light and UVR (Gao et al. 2009; Guan and Gao 2010a, b; Xu et al. 2011, 2016). Although several studies have focused on the haploid phase of this species (mainly on its photosynthesis and interaction with the virus) (Houdan et al. 2005; Frada et al. 2008, 2012; Rokitta and Rost 2012; Mausz and Pohnert 2015; Frada and Vardi 2017; Alexander et al. 2020), little information is available on how UVR affects the haploid phase, which is critical for understanding the ecological niches and the succession of these two phases, especially when both phases coexist during bloom and even the prebloom period (Frada et al. 2012). Therefore, this work aimed to understand the different susceptibilities of photosynthesis of the life-cycle phases to high PAR and UVR.

Materials and methods

Culture conditions

The haploid strain RCC 1217 and the calcifying diploid strain PML B92/11 of *Emiliania huxleyi* were obtained from the Roscoff Culture Collection and originally from coastal waters of Bergen, Norway (Raunefjorden; 60°18.0'N, 05°15.0'E), respectively. The monospecific culture was maintained with an irradiance of 20.8 W m⁻² (100 μmol photons m⁻² s⁻¹) and a 14-h light:10-h dark cycle at 20 °C in AMCONA artificial seawater media (see recipe in Fanesi et al. 2014). For the experiments, semicontinuous cultures were applied; the dilution rates were 0.40 d⁻¹ for the haploid culture and 0.50 d⁻¹ for the diploid culture based on their specific growth rates from batch cultures. The flasks were gently shaken twice daily during the light period to avoid cell sedimentation. Before the experiments, triplicate cultures were allowed to acclimate to the growth conditions for at least eight generations.

Growth rate measurements

To minimize the background counts, sample aliquots from batch cultures were always bubbled with CO₂ for 30 s to remove the coccoliths before cell counting. Cells were enumerated with a Z1 Coulter counter (Beckman Coulter Inc., Indianapolis, Indiana, USA). The

specific growth rate (μ) was calculated using the following formula:

$$\mu = \ln(C_2/C_1)/(t_2 - t_1). \quad (1)$$

C_1 and C_2 represent the cell concentrations at time t_1 and time t_2 , respectively, both of which were at the exponential growth phase (Ruan and Giordano 2017).

Cell size

Haploid or diploid cells in a haemocytometer were checked with an Axioplan 2 Imaging microscope (Zeiss Group, Oberkochen, Germany). Five to eight pictures were randomly taken, and cell diameters were measured by an Auxio Image System (Zeiss Group). The coccolith shell thickness was estimated from the size difference between intact cells (coccolith bearing) and naked cells (coccoliths being removed).

Pigment quantification

Cells were collected by a Whatman GF/F glass fibre filter (General Electronic Company, Boston, Massachusetts, USA) and were placed in 7 ml of 90% acetone at 4 °C overnight. After centrifugation (5000×g, 10 min), the absorption spectrum of the supernatant (400–700 nm) was scanned with a Shimadzu UV-2501 spectrophotometer (Shimadzu Co., Kyoto, Japan), and the chlorophyll *a* and carotenoid contents were calculated according to the following equations (Strickland and Parsons 1972; Jeffrey and Humphrey 1975):

$$\text{chl } a \text{ (mg ml}^{-1}\text{)} = (11.85 \times \text{Abs}_{663-665} - 1.54 \times \text{Abs}_{647} - 0.08 \times \text{Abs}_{630}), \quad (2)$$

$$\text{carotenoids (mg ml}^{-1}\text{)} = 10.0 \times \text{Abs}_{480}, \quad (3)$$

where $\text{Abs}_{663-665}$, Abs_{647} , Abs_{630} , and Abs_{480} represent the absorption values at 663–665 nm, 647 nm, 630 nm, and 480 nm, respectively.

High PAR and UVR exposure under a solar simulator

To assess the responses of different life-cycle phases to acute exposure to the high intensity of PAR and UVR, cultures were dispensed in 20 ml quartz tubes covered with Ultraphan 395 UV opaque foils (Digefra, Munich, Germany) or Ultraphan 295 UV-C cut-off foils (Digefra, Munich, Germany) to obtain the desired light treatments, i.e. PAR alone (irradiance above 395 nm) or PAR+UVR (irradiance above 295 nm). These tubes were incubated in a thermostated bath at growth temperature under a solar simulator (Honle UV Tech., Munich, Germany). The irradiance levels for PAR and UVR were approximately 83.3 W m⁻² (400 μmol photons m⁻² s⁻¹) and 19.0

$W\ m^{-2}$ UVR (18.4 $W\ m^{-2}$ UV-A and 0.63 $W\ m^{-2}$ UV-B), which is similar to the average level of daily intensity. The intensity of solar simulator radiation was recorded with an Eldonet radiometer (Realtime Computer Inc., Mohrendorf, Germany) according to Gao et al. (2009).

Chlorophyll fluorescence measurements

Chlorophyll fluorescence was studied by a Water-PAM fluorometer (Heinz Walz, Pfullingen, Germany). Saturation pulse analysis was used to assess the photosystem yield (Schreiber et al. 1995). After 10 min of darkness, the minimal fluorescence (F_0) was recorded under a weak measuring light ($< 1\ \mu\text{mol photons m}^{-2}\ \text{s}^{-1}$), low enough not to drive the electron flow; the maximum fluorescence (F_m) was subsequently obtained following a saturated pulse (3260 $\mu\text{mol photons m}^{-2}\ \text{s}^{-1}$, pulse width 0.8 s), and the maximum quantum yield was calculated as $F_v/F_m = (F_m - F_0)/F_m$. Similarly, F_m' was excited by the saturated pulse (similar to the F_m measurement) after 20-s exposure to actinic light, which allowed the fluorescence to reach a steady state for all samples; before the application of the saturated pulse when actinic light exposure was going to end, the fluorescence intensity F_t was recorded. The effective quantum yield $\Delta F/F_m'$ was calculated as $(F_m' - F_t)/F_m'$. Non-photochemical quenching (NPQ) was determined based on the equation $\text{NPQ} = (F_m - F_m')/F_m'$. To assess the responses of photosystem II of different life phases to high PAR and UVR stress, $\Delta F/F_m'$ and NPQ were tracked and determined every 5 min for the first 30 min and then every 10 min (Heraud and Beardall 2000; Xing et al. 2015). The repair and damage rates of photosystem II were analysed according to the following equation (Kok 1956; Heraud and Beardall 2000):

$$P/P_{\text{initial}} = (r + k/\exp((k + r)/t))/(k + r). \quad (4)$$

P and P_{initial} represent the effective quantum yields $\Delta F/F_m'$ at time t and the onset of the experiment, respectively; r and k are the repair rate and the damage rate of photosystem II, respectively. To further confirm the effects of high light and UVR on the haploid and diploid photosystems, rapid light curves were recorded in the irradiance range of 0–716 $\mu\text{mol photons m}^{-2}\ \text{s}^{-1}$ with 20 s exposure to each irradiance intensity. rETR, the relative electron transport rate of photosystem II, was estimated using the following equation:

$$\text{rETR} = \Delta F/F_m' \times \text{PFD} \times a \times 0.5, \quad (5)$$

where PFD is the photon flux density, a is the absorption coefficient of chlorophyll a ; and 0.5 represents the factor that accounts for energy partitioning between photosystem II and photosystem I. Since the absorption

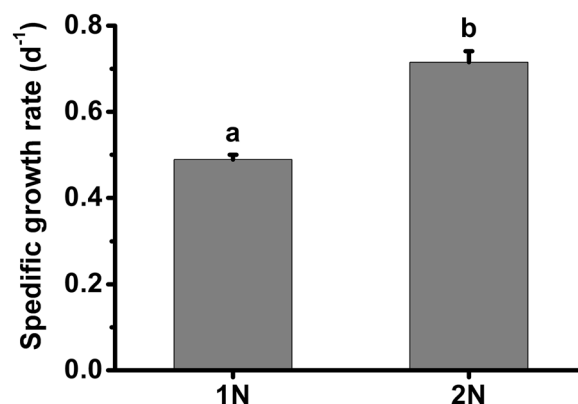


Fig. 1 Growth rate of haploid (1N) and diploid (2N) *Emiliana huxleyi* acclimated to 100 $\mu\text{mol photons m}^{-2}\ \text{s}^{-1}$ at 20 °C. Different superscripted letters indicate significantly different means ($P < 0.05$). Error bars denote standard deviations ($n = 3$)

coefficient was not determined in this work, a constant value of 0.84 was used (Ruan et al. 2018). The rapid light curves were fitted with Origin 7.0 SR0 (OriginLab Co., Northampton, Massachusetts, USA.) according to the following model (Webb et al. 1974):

$$P = P_m \times (1 - \exp(-a \times I/P_m)), \quad (6)$$

where P is the rETR at irradiance I ; P_m is the maximum rETR and a is the maximum quantum efficiency of electron transport.

Statistics

All data were acquired from three independent cultures and are expressed as the mean values with standard deviations. Homogeneity tests for variances were always assessed before further statistical analysis. The significance of variance was then checked by a two-tailed test or two-way ANOVA followed by LSD multiple comparison test by online statistical analysis SPSSAU (V2016-2023, QingSi Technology Ltd, Beijing, China). The significance level was always set at 95%.

Results

The specific growth rates of the haploid and diploid phases were 0.49 d^{-1} and 0.72 d^{-1} , respectively (Fig. 1). Based on these growth rates, daily dilution rates at 0.40 d^{-1} and 0.50 d^{-1} were chosen for the haploid and diploid cultures. After at least eight generations of acclimation to the growth conditions, the cell sizes of various phases were significantly different (Fig. 2). The diploid cells (with coccoliths) were 5.0 μm in diameter, 39% larger than haploid cells (t -test, $P = 0.00 < 0.01$). The coccolith shell around the diploid cell surface was 0.3 μm thick (Fig. 2).

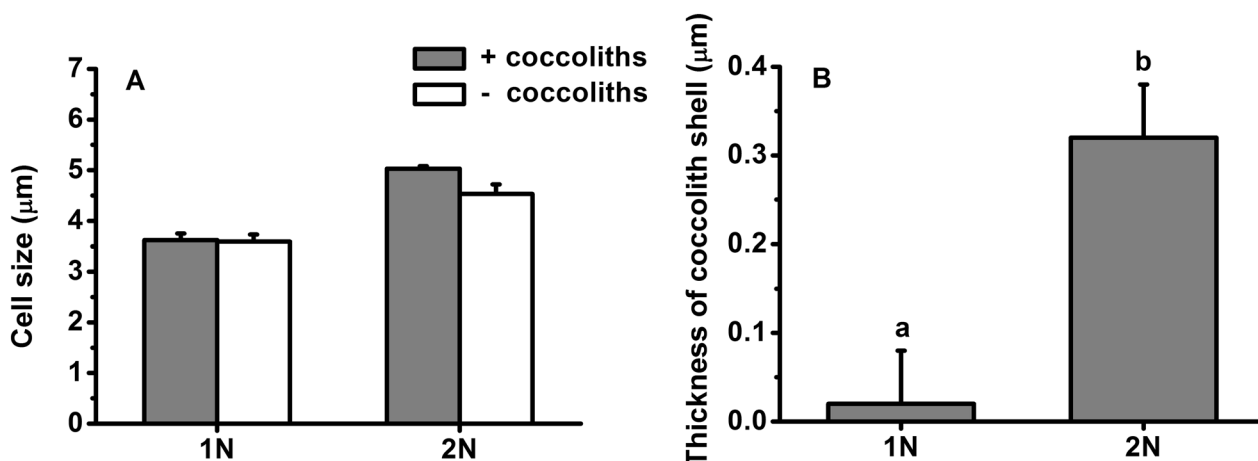


Fig. 2 Cell size (A) and thickness of coccolith shell (B) of haploid (1N) and diploid (2N) *Emiliana huxleyi* acclimated to 100 μmol photons m⁻² s⁻¹ at 20 °C. +Coccoliths and – coccoliths denote the size of cells with and without (removed by bubbling CO₂) coccolith shell. Different letters in superscript indicate significantly different means ($P < 0.05$). Error bars denote standard deviations ($n = 3$)

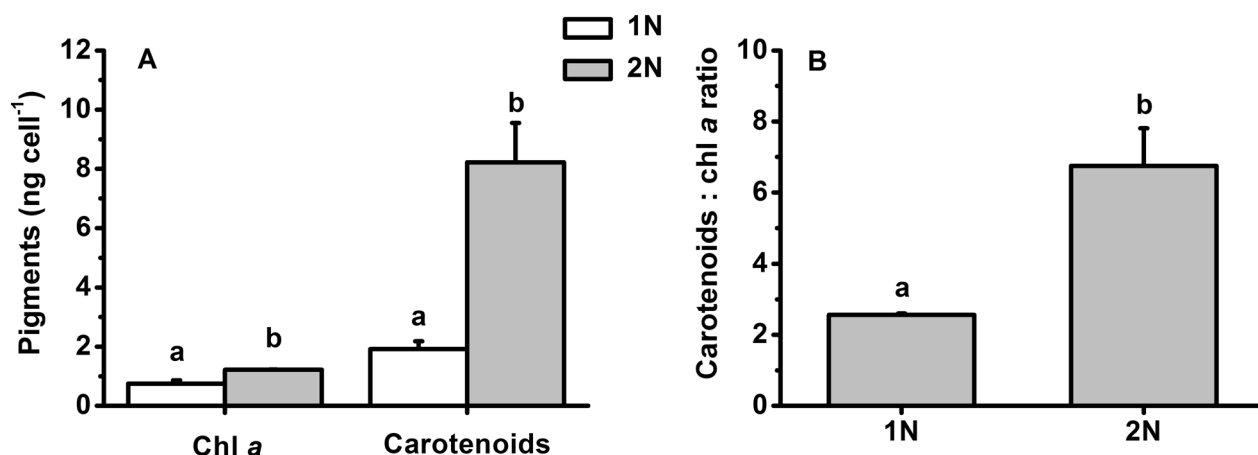


Fig. 3 Pigments content (A) and carotenoid-to-chl *a* ratio (B) of haploid (1N) and diploid (2N) *Emiliana huxleyi* acclimated to 100 μmol photons m⁻² s⁻¹ at 20 °C. Different letters in the superscript indicate significantly different means between different life-cycle phases ($P < 0.05$). Error bars denote standard deviations ($n = 3$)

More pigments (62% for chlorophyll *a* and 328% for carotenoids) were observed in the diploid cells than in the haploid cells (Fig. 3A; *t*-test, $P = 0.00 < 0.01$); when the content of pigments was normalized to cell volume, no difference in chlorophyll *a* was found, yet carotenoids were still 182% more abundant. The carotenoids to chlorophyll *a* ratio of the diploid cells was higher (260%) compared with the haploid cells (Fig. 3B; *t*-test, $P = 0.00 < 0.01$).

When the cultures were exposed to PAR or PAR+UV, the effective quantum yield $\Delta F/F_m'$ decreased drastically in the first 5 min and reached its lowest values in the middle of exposure (25–30 min) for the haploid cells or at the end of the exposure (60 min) for the diploid cells (Fig. 4). Intriguingly, after 60 min of exposure, the effective yield

of the haploid cells under PAR+UVR recovered from the lowest value of 0.22–0.28, a value comparable to that of the PAR treatment (Fig. 4A). Non-photochemical quenching NPQ was always higher in haploid cultures than in their counterparts, as is especially evident for those cultures exposed to PAR+UVR. NPQ reached its maximum value after 40 min for the haploid cultures and 30 min for the diploid cultures (Fig. 4C, D).

Although there was no significant difference in the repair rates (*r*) of photosystem II between different phases ($F_{(1,8)} = 1.13$, $P = 0.32 > 0.05$) or radiation treatments ($F_{(1,8)} = 0.20$, $P = 0.67 > 0.05$), the damage rates (*k*) of photosystem II in the diploid cells were approximately 59–60% lower than those of their haploid counterparts ($F_{(1,8)} = 52.29$, $P = 0.00 < 0.05$). The *r*/*k* ratios of the diploid

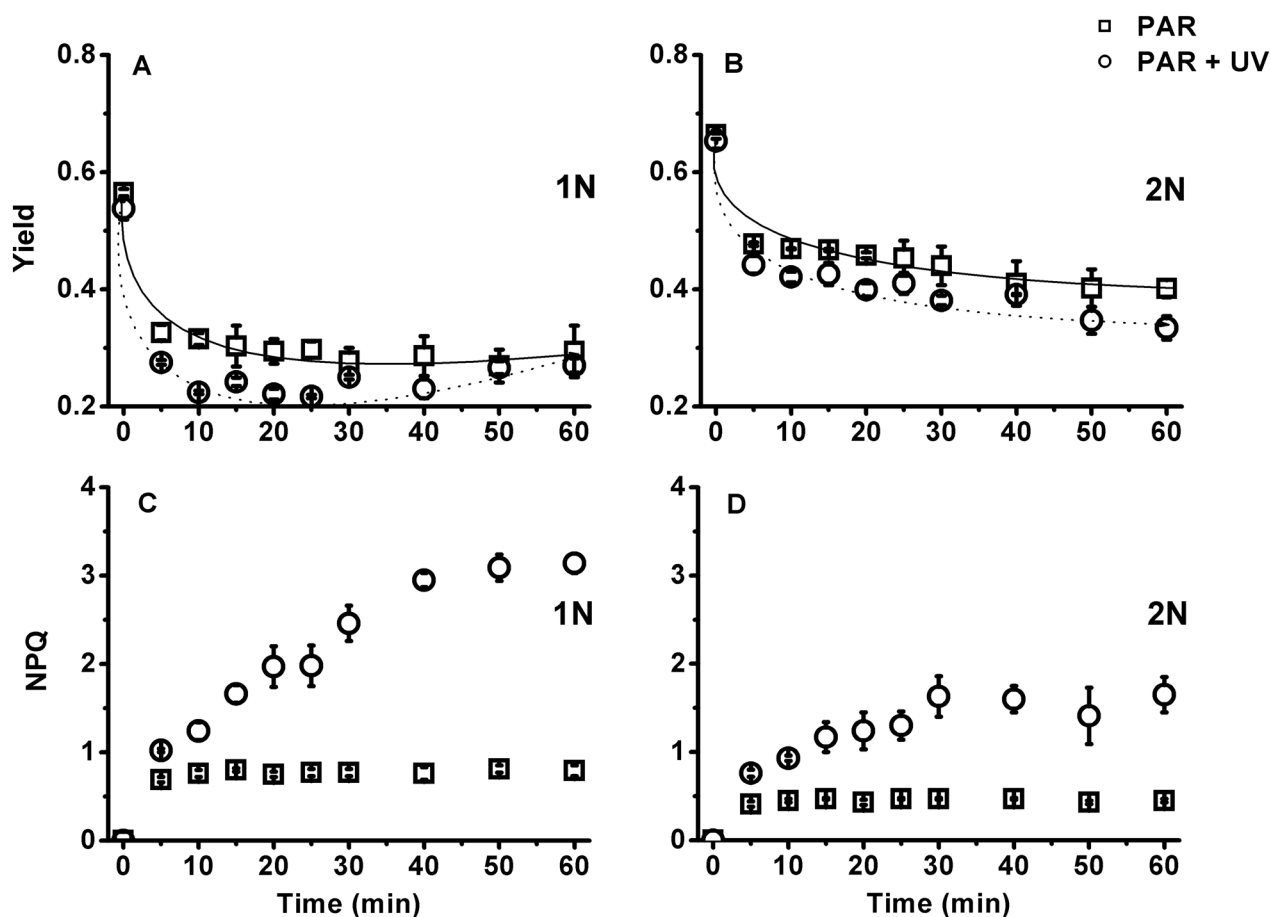


Fig. 4 Dynamic changes in effective quantum yield (A, B) and nonphotochemical quenching (NPQ) (C, D) of haploid (1N) and diploid (2N) *Emiliana huxleyi* under a solar radiation simulator with 83.3 W m⁻² PAR (400 μmol photons m⁻² s⁻¹) and 19.0 W m⁻² UVR. Error bars denote standard deviations (n=3)

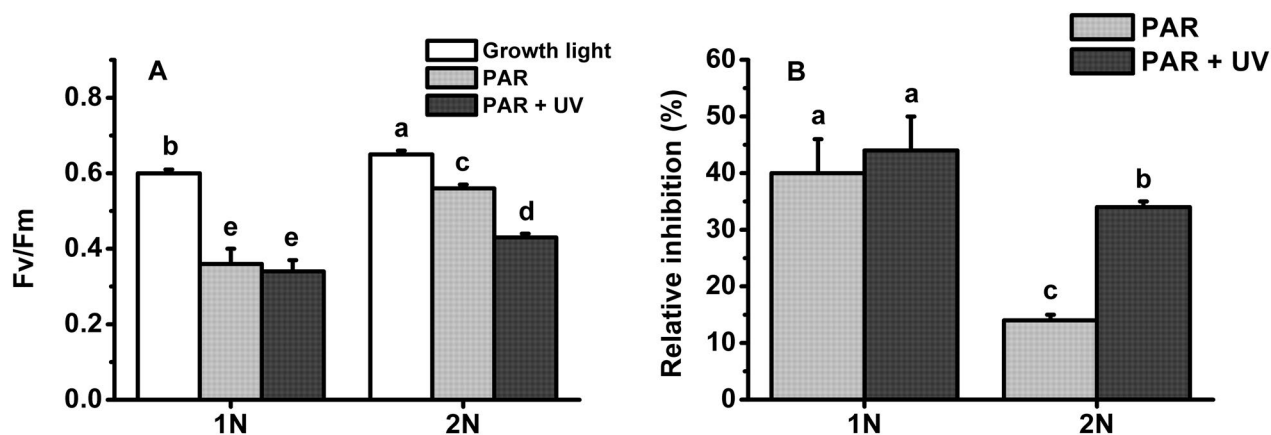


Fig. 5 A Maximum quantum yield of haploid (1N) and diploid (2N) *Emiliana huxleyi* after acclimation to growth light or 1 h of acute exposure to PAR or PAR + UVR. B Relative inhibition of F_v/F_m induced by PAR or PAR + UVR. The growth light, PAR and UVR were 20.8 W m⁻² (100 μmol photons m⁻² s⁻¹), 83.3 W m⁻² (400 μmol photons m⁻² s⁻¹) and 19.0 W m⁻², respectively. Error bars denote standard deviations (n=3). Different letters represent significantly different means between different life-cycle phases and different radiation treatments ($P < 0.05$)

cells were 1.5–1.7, whereas those of the haploid cells were lower than or close to 1.

To confirm the insensitivity of the haploid cells to UVR exposure, the maximum quantum yield (F_v/F_m) was determined after exposure to the solar simulator. F_v/F_m between the haploid cells treated with PAR alone and with PAR+UVR was comparable (Fig. 5), and the relative inhibition rates (taking cultures maintained at growth light as a control) were 40% for the PAR treatments and 44% for the PAR+UVR treatments. However, the relative inhibition of F_v/F_m caused by PAR+UVR was approximately 2.4-fold higher than by PAR alone in the diploid cells.

The photosynthesis parameters of the rapid light curves further confirmed the results of the previous experiment. The maximum relative electron transport rates ($rETR_{max}$) of the haploid cells were significantly lower (34–39%) under the solar simulator than those acclimated to growth light (t-test, $P=0.00 < 0.05$), although no significant difference in $rETR_{max}$ was found between the PAR and PAR+UVR treatments (Table 2). No inhibition of $rETR_{max}$ in the diploid cultures was caused by PAR alone, but PAR plus UVR resulted in 34% inhibition. The slope of the linear part of the curve (a) of the haploid cultures was more sensitive to high light exposure than that of the haploid cells: the relative inhibitions (compared with those maintained at growth light) were 16% (PAR) – 31% (PAR+UVR) for the haploid cultures and 3% (PAR) – 24% (PAR+UVR) for the diploid cultures (Table 2). The saturation irradiance (E_k) was not affected by radiation (PAR or PAR+UVR; $F_{(2,12)}=3.23$, $P=0.07 > 0.05$), except for the haploid cultures exposed to PAR alone.

Table 1 Repair rate (r) and damage rate (k) of photosystem II obtained from effective quantum yield dynamics of haploid (1N) and diploid (2N) *Emiliania huxleyi* during 1 h of acute exposure to PAR or PAR+UVR under a solar radiation simulator according to Heraud and Beardall (2000)

	1N		2N	
	PAR	PAR+UVR	PAR	PAR+UVR
Repair rate (r)	0.19±0.03 ^a	0.20±0.01 ^a	0.12±0.06 ^a	0.14±0.02 ^a
Damage rate (k)	0.18±0.03 ^b	0.24±0.01 ^a	0.07±0.02 ^c	0.10±0.02 ^c
r/k ratio	1.06±0.02 ^b	0.84±0.06 ^c	1.67±0.28 ^a	1.48±0.10 ^a

PAR and UVR were 83.3 W m⁻² (400 μmol photons m⁻² s⁻¹) and 19.0 W m⁻², respectively. The values are shown as the mean ± standard deviation ($n=3$). Different letters denote significantly different means between different life-cycle phases and radiation treatments ($P < 0.05$)

Discussion

The haploid and diploid phases of *E. huxleyi* have marked morphological differences and share only half of the transcripts in common at the exponential stage, resulting in divergent physiologies in carbon and nutrient uptake and assimilation, energy budget, and biomass accumulation (Rokitta et al. 2011, 2012; Rokitta and Rost 2012; Alexander et al. 2020). It is, therefore, not surprising that the photosynthesis and the growth rate of these two phases were different (Fig. 1; Table 2), which were also reported previously (Houdan et al. 2005; Rokitta and Rost 2012; Mausz and Pohnert 2015). Moreover, the photosynthesis of haploid cells seemed to be more sensitive to the high PAR intensity but resistant to UVR-induced inhibition compared with the diploid counterparts (Figs. 4, 5, 6; Table 2).

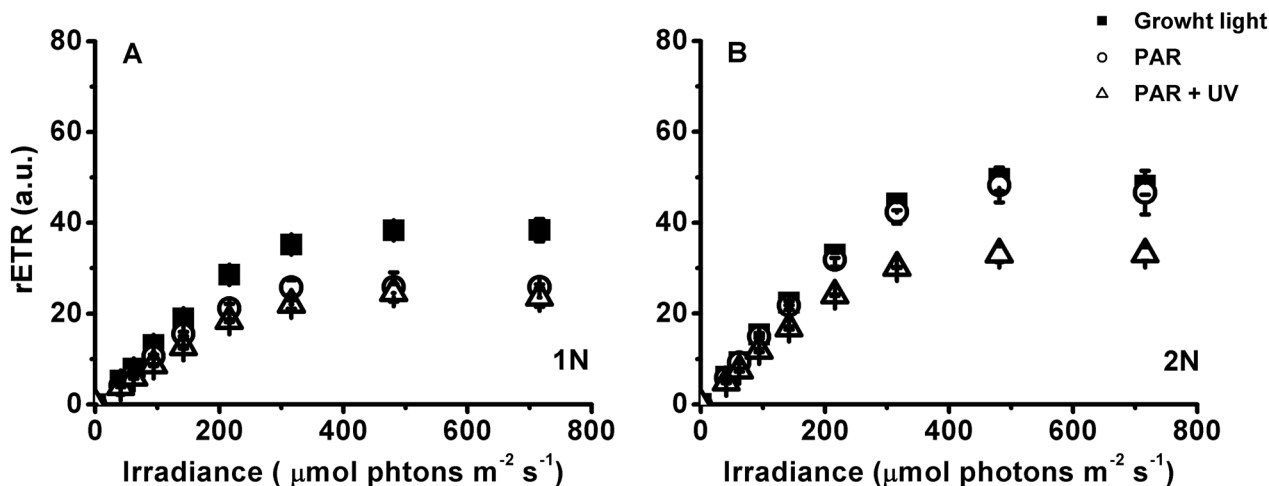


Fig. 6 Rapid light curves of haploid (1N) and diploid (2N) *Emiliania huxleyi* after acclimation to growth light or 1 h of acute exposure to PAR or PAR+UVR. The growth light, PAR and UVR were 20.8 W m⁻² (100 μmol photons m⁻² s⁻¹), 83.3 W m⁻² (400 μmol photons m⁻² s⁻¹) and 19.0 W m⁻², respectively. Error bars denote standard deviations ($n=3$)

Table 2 Parameters of the relative electron transport rate (rETR) versus irradiance curves of haploid (1N) and diploid (2N) *Emiliania huxleyi* after acclimation to growth light or 1 h of acute exposure to PAR or PAR + UVR

	1N			2N		
	Growth light	PAR	PAR + UVR	Growth light	PAR	PAR + UVR
rETR _{max}	42.4 ± 2.6 ^b	27.8 ± 1.9 ^d	26.0 ± 2.5 ^d	54.7 ± 2.8 ^a	53.1 ± 5.8 ^a	36.2 ± 2.2 ^c
a	0.19 ± 0.01 ^b	0.16 ± 0.01 ^c	0.14 ± 0.01 ^d	0.22 ± 0.00 ^a	0.22 ± 0.01 ^a	0.17 ± 0.01 ^c
E _k	221 ± 21 ^a	173 ± 5 ^b	199 ± 28 ^{ab}	245 ± 10 ^a	245 ± 21 ^a	215 ± 24 ^a

The growth light, PAR and UVR were 20.8 W m⁻² (100 μmol photons m⁻² s⁻¹), 83.3 W m⁻² (400 μmol photons m⁻² s⁻¹) and 19.0 W m⁻², respectively. rETR_{max} maximum relative electron transport rate; a, slope of the light-limited portion of the rETR versus irradiance curve; E_k (μmol photons m⁻² s⁻¹), the irradiance at which energy becomes saturated for electron transport. The values are shown as the mean ± standard deviation (n = 3). Different letters denote significantly different means between different life-cycle phases and radiation treatments (P < 0.05)

Under supersaturating light, the diploid cells showed less photoinhibition than the haploid cells, which may be associated with a discrepancy in the capability of dissipating excess energy and subsequent production of reactive oxygen species that damage pigments and proteins and affect the structure and activity of photosystems (Foyer and Harbinson 1999; Shi et al. 2020). As one of the major sinks of cell energy, calcification is important in excess energy dissipation (e Ramos et al. 2012; Monteiro et al. 2016; Zhang and Gao 2021). The energy budget of calcification (including calcium transport, bicarbonate transport, polysaccharide generation, etc.) might account for up to 37% of the total photosynthetic energy (Monteiro et al. 2016). In particular, an abrupt increase in light intensity could cause an 11-fold increase in calcification with only a 5-fold increase in photosynthesis (e Ramos et al. 2012). That is, calcification may consume as much as 81% of the total photosynthesis energy, given that calcification and photosynthesis are operating at a comparable rate (Lorenzo et al. 2019). Calcification may therefore contribute to at least partly excess energy dissipation since the damage rate of photosystem II in the diploid cells was lower (Table 1). In addition, the calcareous shell formed by coccoliths also absorbs and/or attenuates a significant proportion of PAR (Gao et al. 2009). This may further alleviate high PAR stress. Although the coccosphere may remove up to 20% of PAR, the coccosphere in the present study is too thin (only 0.3 μm) and could reduce only 3% of solar irradiance based on our previous study (Fig. 2; Ruan et al. 2016). Therefore coccoliths *per se* in the present study might have a very limited contribution to photoprotection. In addition to calcification and coccolith shell, carotenoids often play a role in light harvesting or energy dissipation depending on the light availability (Goss and Lepetit 2015; Leverenz et al. 2015; Xi et al. 2022), and they were higher in the diploid cells (Fig. 3). Potentially, these calcified cells could be more active in dissipating energy via the xanthophyll cycle

when subjected to supersaturated light. However, the NPQ values in our study did not seem to support this, as may be related to the fact that calcification was the main player in consuming excess energy. Thus, the less effective NPQ was actually an indication of less stress under high light, manifested by the lower damage rate in the diploid cells (Table 1), whereas the NPQ of the haploid cells could be the main path to disperse excess energy.

The presence of UVR led to a further decrease of quantum yield in the haploid cells compared with PAR alone. Intriguingly, this decrease completely recovered at the end of the exposure (Fig. 4), which was further confirmed by F_v/F_m and other photosynthetic parameters (Fig. 6; Table 2). One of the reasons for this recovery may be attributed to the haploid cells being very active in repair and protein turnover (Table 1; Rokitta et al. 2011). Since no similar recovery was also observed under PAR alone, the enhanced repair in the haploid cells could be partly activated by UV-A/B. The UV-specific photoreceptor UV Resistance Locus 8 (UVR8) in the cytosol can be the candidate for this activation (Tilbrook et al. 2016). Upon UV exposure, UVR8 monomerizes to its active form and interacts with E3 ubiquitin ligase constitutively photomorphogenic 1 (COP1) in the nucleus to form the UVR8-COP1 complex (Tokutsu et al. 2021; Wang et al. 2022), which will change the expression of a serial of genes, e.g. D1 protein, to expedite the repair process and thus the recovery of quantum yield (Tilbrook et al. 2016; Giovagnetti and Ruban 2018). What's more, two critical proteins LHCSR1 (photoprotective proteins LHC stress-related protein 1) and PsbS (photosystem II subunit S) contributing to NPQ can also be induced by UV exposure (Allorant et al. 2016), which may explain the sharp increase in NPQ of both haploidic and diploidic cells treated with UV. It is, however, noteworthy that a complete UVR8-COP1 signalling pathway has not been identified by far in the red lineage (e.g. diatom, coccolithophore) (Giovagnetti and Ruban 2018); whether this anterograde regulation also functions in coccolithophores is yet to

be verified. Unlike haploid cells, the diploid cells were susceptible to UVR-induced inhibition: the damage rate of photosystem II increased by 43% (Fig. 6; Table 1). In addition, calcification is also very sensitive to UVR. In our previous study, calcification could be reduced by up to 44% under a similar level of UVR (Gao et al. 2009). Therefore, the reduction in calcification constrained excess energy dissipation and exacerbated the UVR stress that the diploid cells encountered.

Although the vertical distribution of the haploid phase of *E. huxleyi* is still unclear due to the lack of distinguishable coccolith, different photosynthetic responses of the haploid and diploid phases to acute exposure to high irradiance imply various ecological niches they occupy. The diploid phase tends to distribute even bloom in the surface water, where the light can be up to 1500 $\mu\text{mol photons m}^{-2} \text{ s}^{-1}$, because of the exceptional tolerance of high light. The haploid phase can recover from UVR-induced inhibition, as is important for this phase to immediately regain and maintain a relatively high photosynthesis in a variable environment of the surface seawater, e.g. during the process of the vertical mix. However, the photosynthesis of the haploid phase is in general more susceptible to high irradiance than the diploid phase, regardless of UVR. This implies that haploid *E. huxleyi* may thus tend to inhabit the relatively low part of the water column.

Abbreviations

1N	Haploid phase
2N	Diploid phase
F_v/F_m	Maximum quantum yield
NPQ	Non-photochemical quenching
PAR	Photosynthetically active radiation
UVR	Ultraviolet radiation
$\Delta F/F_m'$	Effective quantum yield
μ	Specific growth rate

Acknowledgements

The authors are grateful to the funding support.

Author contributions

The authors confirm contribution to the paper as follows: study conception and design: ZR; data collection: ML and ZR; analysis and interpretation of results: ZR and DQ; HX; draft manuscript preparation: ZR, DQ, HX, HL, SC, PL and WC. All authors reviewed the results and approved the final version of the manuscript.

Funding

This work was funded by the National Key Research and Development Program (2019YFB1503904), National Natural Science Foundation of China (42076206), Guangdong Basic and Applied Basic Research Foundation (2020A1515011073, 2016A030313066) and Department of Science and Technology of Guangdong Province (2021B1212050025 and STKJ2021125).

Availability of data and materials

The datasets used and/or analysed during the current study are available from the corresponding author on reasonable request.

Declarations

Ethics approval and consent to participate

Not applicable.

Consent for publication

Not applicable.

Competing interests

The authors declare they have no competing interests.

Author details

¹STU-UNIVPM Joint Algal Research Center, Guangdong Provincial Key Laboratory of Marine Biotechnology, Marine Biology Institute, Shantou University, Shantou 515063, Guangdong, China. ²CAS Key Laboratory of Renewable Energy, Guangzhou Institute of Energy Conversion, Chinese Academy of Sciences, Guangzhou 510640, Guangdong, China. ³CAS Key Laboratory of Tropical Marine Bio-Resources and Ecology, South China Sea Institute of Oceanology, Chinese Academy of Sciences, Guangzhou 510301, Guangdong, China. ⁴Southern Marine Science and Engineering Guangdong Laboratory (Guangzhou), Guangzhou 511458, Guangdong, China. ⁵College of Pharmacy and Life Sciences, Jiujiang University, Jiujiang 332005, Jiangxi, China.

Received: 23 February 2023 Accepted: 15 June 2023

Published online: 14 July 2023

References

- Alexander H, Rouco M, Haley ST, Dyhrman ST (2020) Transcriptional response of *Emiliania huxleyi* under changing nutrient environments in the North Pacific Subtropical Gyre. *Environ Microbiol* 22:1847–1860
- Allouret G, Lefebvre-Legendre L, Chappuis R, Kuntz M, Truong TB, Niyogi KK, Ulm R, Goldschmidt-Clermont M (2016) UV-B photoreceptor-mediated protection of the photosynthetic machinery in *Chlamydomonas reinhardtii*. *Proc Natl Acad Sci U S A* 113:14864–14869
- Anning T, Nimer N, Merrett M, Brownlee C (1996) Costs and benefits of calcification in coccolithophorids. *J Mar Syst* 9:45–56
- Balch W, Drapeau D, Bowler B, Booth E (2007) Prediction of pelagic calcification rates using satellite measurements. *Deep Sea Res (II Top Stud Oceanogr)* 54:478–495
- Boelen P, Obernosterer I, Vink AA, Buma AG (1999) Attenuation of biologically effective UV radiation in tropical Atlantic waters measured with a biochemical DNA dosimeter. *Photochem Photobiol* 69:34–40
- Brown CW, Yoder JA (1994) Coccolithophorid blooms in the global ocean. *J Geophys Res (c Oceans)* 99:7467–7482
- Brownlee C, Langer G, Wheeler GL (2021) Coccolithophore calcification: changing paradigms in changing oceans. *Acta Biomater* 120:4–11
- Buma AG, Van Oijen T, Van De Poll W, Veldhuis MJ, Gieskes WW (2000) The sensitivity of *Emiliania huxleyi* (Prymnesiophyceae) to ultraviolet-B radiation. *J Phycol* 36:296–303
- D'Amario B, Ziveri P, Grelaud M, Oviedo A, Kralj M (2017) Coccolithophore haploid and diploid distribution patterns in the Mediterranean Sea: can a haplo-diploid life cycle be advantageous under climate change? *J Plankton Res* 39:781–794
- de Vries J, Monteiro F, Wheeler G, Poulton A, Godrijan J, Cerino F, Malinverno E, Langer G and Brownlee C (2020) The haplo-diplontic life cycle expands niche space of coccolithophores. *Biogeosci Disc*: 1–39.
- Falkowski PG, Raven JA (1997) Light absorption and energy transfer in the photosynthetic apparatus. In: Falkowski PG, Raven JA (eds). *Aquatic photosynthesis*. Blackwell Science, Malden MA. Princeton University Press, Princeton, pp 33–64
- Fanesi A, Raven JA, Giordano M (2014) Growth rate affects the responses of the green alga *Tetraselmis suecica* to external perturbations. *Plant, Cell Environ* 37:512–519
- Foyer CH, Harbinson J (1999) Relationships between antioxidant metabolism and carotenoids in the regulation of photosynthesis. In: Frank HA, Young AJ, Britton G, Cogdell RJ (eds) *The photochemistry of carotenoids*. Kluwer Academic Publishers, London, pp 305–325

- Frada M, Vardi A (2017) Morphological switch to a resistant subpopulation in response to viral infection in a bloom-forming marine microalgae. *PLoS Path* 13:e1006775
- Frada M, Probert I, Allen MJ, Wilson WH, de Vargas C (2008) The “Cheshire Cat” escape strategy of the coccolithophore *Emiliana huxleyi* in response to viral infection. *Proc Natl Acad Sci* 105:15944–15949
- Frada MJ, Bidle KD, Probert I, de Vargas C (2012) *In situ* survey of life cycle phases of the coccolithophore *Emiliana huxleyi* (Haptophyta). *Environ Microbiol* 14:1558–1569
- Gao K, Ruan Z, Villafane VE, Gattuso J-P, Helbling EW (2009) Ocean acidification exacerbates the effect of UV radiation on the calcifying phytoplankter *Emiliana huxleyi*. *Limnol Oceanogr* 54:1855–1862
- Giovagnetti V, Ruban AV (2018) The evolution of the photoprotective antenna proteins in oxygenic photosynthetic eukaryotes. *Biochem Soc Trans* 46:1263–1277
- Goss R, Lepetit B (2015) Biodiversity of NPQ. *J Plant Physiol* 172:13–32
- Green J, Course P, Tarran G (1996) The life-cycle of *Emiliana huxleyi*: a brief review and a study of relative ploidy levels analysed by flow cytometry. *J Mar Syst* 9:33–44
- Guan W, Gao K (2010a) Enhanced calcification ameliorates the negative effects of UV radiation on photosynthesis in the calcifying phytoplankter *Emiliana huxleyi*. *Chin Sci Bull* 55:588–593
- Guan W, Gao K (2010b) Impacts of UV radiation on photosynthesis and growth of the coccolithophore *Emiliana huxleyi* (Haptophyceae). *Environ Exp Bot* 67:502–508
- Haney AM, Sanfilippo JE, Garczarek L, Partensky F, Kehoe DM (2022) Multiple photolyases protect the marine cyanobacterium *Synechococcus* from ultraviolet radiation. *Mbio* 13:e01511-e1522
- Heraud P, Beardall J (2000) Changes in chlorophyll fluorescence during exposure of *Dunaliella tertiolecta* to UV radiation indicate a dynamic interaction between damage and repair processes. *Photosynthesis Res* 63:123–134
- Holligan PM, Fernández E, Aiken J, Balch WM, Boyd P, Burkill PH, Finch M, Groom SB, Malin G, Muller K (1993) A biogeochemical study of the coccolithophore, *Emiliana huxleyi*, in the North Atlantic. *Global Biogeochem Cycles* 7:879–900
- Houdan A, Probert I, Van Lenning K, Lefebvre S (2005) Comparison of photosynthetic responses in diploid and haploid life-cycle phases of *Emiliana huxleyi* (Prymnesiophyceae). *Mar Ecol Prog Ser* 292:139–146
- Jeffrey S, Humphrey G (1975) New spectrophotometric equations for determining chlorophylls a, b, c1 and c2 in higher plants, algae and natural phytoplankton. *Biochem Physiol Pflanz* 167:191–194
- Jin P, Gao K, Villafañe VE, Campbell DA, Helbling W (2013) Ocean acidification alters the photosynthetic responses of a coccolithophorid to fluctuating UV and visible radiation. *Plant Physiol* 162:2084–2094
- Jin P, Wan J, Zhang J, Overmans S, Xiao M, Ye M, Dai X, Zhao J, Gao K, Xia J (2022) Additive impacts of ocean acidification and ambient ultraviolet radiation threaten calcifying marine primary producers. *Sci Total Environ* 818:151782
- Kayano K, Shiraiwa Y (2009) Physiological regulation of coccolith polysaccharide production by phosphate availability in the coccolithophorid *Emiliana huxleyi*. *Plant Cell Physiol* 50:1522–1531
- Kayano K, Saruwatari K, Kogure T, Shiraiwa Y (2011) Effect of coccolith polysaccharides isolated from the coccolithophorid, *Emiliana huxleyi*, on calcite crystal formation in *in vitro* CaCO₃ crystallization. *Mar Biotechnol* 13:83–92
- Kok B (1956) On the inhibition of photosynthesis by intense light. *Biochimica Et Biophysica Acta* 21:234–244
- Leunert F, Eckert W, Paul A, Gerhardt V, Grossart H-P (2014) Phytoplankton response to UV-generated hydrogen peroxide from natural organic matter. *J Plankton Res* 36:185–197
- Leverenz RL, Sutter M, Wilson A, Gupta S, Thurotte A, de Carbon CB, Petzold CJ, Ralston C, Perreau F, Kirilovsky D (2015) A 12 Å carotenoid translocation in a photoswitch associated with cyanobacterial photoprotection. *Science* 348:1463–1466
- Lorenzo MR, Neale PJ, Sobrino C, León P, Vázquez V, Bresnan E, Segovia M (2019) Effects of elevated CO₂ on growth, calcification, and spectral dependence of photoinhibition in the coccolithophore *Emiliana huxleyi* (Prymnesiophyceae). *J Phycol* 55:775–788
- Mausz MA, Pohnert G (2015) Phenotypic diversity of diploid and haploid *Emiliana huxleyi* cells and of cells in different growth phases revealed by comparative metabolomics. *J Plant Physiol* 172:137–148
- Monteiro FM, Bach LT, Brownlee C, Bown P, Rickaby RE, Poulton AJ, Tyrrell T, Beaufort L, Dutkiewicz S, Gibbs S (2016) Why marine phytoplankton calcify. *Sci Adv* 2:e1501822
- Nanninga H, Tyrrell T (1996) Importance of light for the formation of algal blooms by *Emiliana huxleyi*. *Mar Ecol Prog Ser* 136:195–203
- Pozdnyakov DV, Gnatiuk NV, Davy R, Bobylev LP (2021) The phenomenon of *Emiliana huxleyi* in aspects of global climate and the ecology of the world ocean. *Geogr Environ Sustain* 14:50–62
- Ramos JB, Schulz KG, Febiri S, Riebesell U (2012) Photoacclimation to abrupt changes in light intensity by *Phaeodactylum tricornutum* and *Emiliana huxleyi*: the role of calcification. *Mar Ecol Prog Ser* 452:11–26
- Rokitta SD, Rost B (2012) Effects of CO₂ and their modulation by light in the life-cycle stages of the coccolithophore *Emiliana huxleyi*. *Limnol Oceanogr* 57:607–618
- Rokitta SD, de Nooijer LJ, Trimborn S, de Vargas C, Rost B, John U (2011) Transcriptome analyses reveal differential gene expression patterns between the life-cycle stages of *Emiliana huxleyi* (haptophyta) and reflect specialization to different ecological niches. *J Phycol* 47:829–838
- Rokitta SD, John U, Rost B (2012) Ocean acidification affects redox-balance and ion-homeostasis in the life-cycle stages of *Emiliana huxleyi*. *PLoS ONE* 7:e52212
- Ruan Z, Giordano M (2017) The use of NH₄⁺ rather than NO₃⁻ affects cell stoichiometry, C allocation, photosynthesis and growth in the cyanobacterium *Synechococcus* sp. UTEX LB 2380, only when energy is limiting. *Plant, Cell Environ* 40:227–236
- Ruan Z, Zou D, Xu Z, Deng Y, Wang T, Huang F, Luo L (2016) Cocosphere relieves the stress of ultraviolet radiation on photosynthesis in the coccolithophorid *Emiliana huxleyi*. *Acta Hydrobiol Sin* 40:1078–1082
- Ruan Z, Prášil O, Giordano M (2018) The phycobilisomes of *Synechococcus* sp. are constructed to minimize nitrogen use in nitrogen-limited cells and to maximize energy capture in energy-limited cells. *Environ Exp Bot* 150:152–160
- Schreiber U, Endo T, Mi H, Asada K (1995) Quenching analysis of chlorophyll fluorescence by the saturation pulse method: particular aspects relating to the study of eukaryotic algae and cyanobacteria. *Plant Cell Physiol* 36:873–882
- Shi D, Zhuang K, Chen Y, Xu F, Hu Z, Shen Z (2020) Effects of excess ammoniacal nitrogen (NH₄⁺-N) on pigments, photosynthetic rates, chloroplast ultrastructure, proteomics, formation of reactive oxygen species and enzymatic activity in submerged plant *Hydrilla verticillata* (Lf) Royle. *Aquat Toxicol* 226:105585
- Sinha RP, Häder D-P (2002) UV-induced DNA damage and repair: a review. *Photochem Photobiol Sci* 1:225–236
- Strickland JDH, Parsons TR (1972) A practical handbook of seawater analysis. *Bull Fisheries Res Board Canada* 167:310
- Tilbrook K, Dubois M, Crocco CD, Yin R, Chappuis R, Allorent G, Schmid-Siegert E, Goldschmidt-Clermont M, Ulm R (2016) UV-B perception and acclimation in *Chlamydomonas reinhardtii*. *Plant Cell* 28:966–983
- Tokutsu R, Fujimura-Kamada K, Yamasaki T, Okajima K, Minagawa J (2021) UV-A/B radiation rapidly activates photoprotective mechanisms in *Chlamydomonas reinhardtii*. *Plant Physiol* 185:1894–1902
- Tyrrell T, Merico A (2004) *Emiliana huxleyi*: bloom observations and the conditions that induce them. In: Thierstein HR, Young JR (eds) *Coccolithophores: from molecular processes to global impact*. Springer, Berlin, pp 75–97
- van Rijssel M, Buma AG (2002) UV radiation induced stress does not affect DMSP synthesis in the marine prymnesiophyte *Emiliana huxleyi*. *Aquat Microb Ecol* 28:167–174
- Vázquez V, León P, Gordillo FJ, Jiménez C, Concepción I, Mackenzie K, Bresnan E and Segovia M (2022) High-CO₂ levels rather than acidification restrict *Emiliana huxleyi* growth and performance. *Microb Ecol*: 1–17.
- Wang Y, Wang L, Guan Z, Chang H, Ma L, Shen C, Qiu L, Yan J, Zhang D, Li J (2022) Structural insight into UV-B-activated UVR8 bound to COP1. *Sci Adv* 8:eabn3337
- Webb WL, Newton M, Starr D (1974) Carbon dioxide exchange of *Alnus rubra*. *Oecologia* 14:281–291
- Xi Y, Bian J, Luo G, Kong F, Chi Z (2022) Enhanced β-carotene production in *Dunaliella salina* under relative high flashing light. *Algal Res* 67:102857
- Xing T, Gao K, Beardall J (2015) Response of growth and photosynthesis of *Emiliana huxleyi* to visible and UV irradiances under different light regimes. *Photochem Photobiol* 91:343–349

- Xu K, Gao K, Villafañe V, Helbling E (2011) Photosynthetic responses of *Emiliania huxleyi* to UV radiation and elevated temperature: roles of calcified coccoliths. *Biogeosciences* 8:1441–1452
- Xu J, Bach LT, Schulz KG, Zhao W, Gao K, Riebesell U (2016) The role of coccoliths in protecting *Emiliania huxleyi* against stressful light and UV radiation. *Biogeosciences* 13:4637–4643
- Zang S, Xu Z, Yan F, Wu H (2022) Elevated CO₂ modulates the physiological responses of *Thalassiosira pseudonana* to ultraviolet radiation. *J Photochem Photobiol B: Biol* 236:112572
- Zhang Y, Gao K (2021) Photosynthesis and calcification of the coccolithophore *Emiliania huxleyi* are more sensitive to changed levels of light and CO₂ under nutrient limitation. *J Photochem Photobiol b: Biol* 217:112145
- Zondervan I (2007) The effects of light, macronutrients, trace metals and CO₂ on the production of calcium carbonate and organic carbon in coccolithophores—a review. *Deep Sea Res (II Top Stud Oceanogr)* 54:521–537

Publisher's Note

Springer Nature remains neutral with regard to jurisdictional claims in published maps and institutional affiliations.

Submit your manuscript to a SpringerOpen[®] journal and benefit from:

- ▶ Convenient online submission
- ▶ Rigorous peer review
- ▶ Open access: articles freely available online
- ▶ High visibility within the field
- ▶ Retaining the copyright to your article

Submit your next manuscript at ▶ [springeropen.com](https://www.springeropen.com)
